



## Low-Field Mobility and Quantum Effects in Asymmetric Silicon-Based Field-Effect Devices

I. KNEZEVIC, D. VASILESKA, X. HE, D.K. SCHRODER AND D.K. FERRY

*Department of Electrical Engineering and Center for Solid State Electronics Research, Arizona State University, Tempe, AZ 85287-5706, USA*

irenak@asu.edu

**Abstract.** Though asymmetric MOSFET structures are being designed in response to small-geometry effects, the performance estimates of such devices often rely on the conventional device description, and neglect to properly account for the interplay between quantum effects and the effects of asymmetry. In this paper, we investigate the low-field transport in a highly asymmetric MOSFET structure, characterized by a  $p^+$ -implant at the source end, by using a Monte Carlo—Poisson simulation with the quantum effects incorporated through an effective potential. We observe that highly-pronounced asymmetry leads to ballistic transport features, which become suppressed by the inclusion of quantum effects. We prove that mobility degradation is an essentially non-equilibrium signature of quantum mechanics, independent of the well-established equilibrium signatures (charge set-back and gap widening). Consequently, in order to properly estimate the device performance, it becomes important to account for the channel mobility degradation due to quantum effects.

**Keywords:** low-field transport, electron mobility, Monte Carlo simulation, asymmetric structures

### 1. Introduction

Asymmetrically doped metal-oxide-semiconductor field-effect transistors (MOSFETs) have recently received much attention due to the current quest to optimize the transistor performance simultaneously with its continuing shrinking, and overcome the inevitable accompanying increase in the severity of small-geometry effects. Representative asymmetric structures, which show improved performance with respect to some of the detrimental small-geometry effects, include the lightly-doped drain (LDD) devices, gate overlapped LDD structures (GOLD), halo source GOLD drain (HS-GOLD) (Buti *et al.* 1991), graded-channel MOSFETs (GCMOS) (Ma *et al.* 1997), and focused-ion-beam MOSFETs (FIBMOS) (Shen *et al.* 1998, Kang and Schroder 2000, Kang *et al.* in press). However, very often the performance of these devices is predicted according to models that hold for conventional MOSFETs, which are inadequate for several reasons. First, unlike conventional MOSFETs,

these devices are small and are therefore expected to experience quantum transport under bias. Secondly, the optimized doping profiles of such devices produce highly inhomogeneous electric fields, which may lead to non-stationary transport features, like velocity overshoot, even under steady-state conditions. The interplay between the small and the asymmetric has not been fully understood yet, but it certainly holds promise for some new and exciting transport phenomena.

In this paper, we present the results of a Monte Carlo particle-based simulation of low-field transport in an asymmetric MOSFET structure, with quantum effects included through an effective potential (Ferry 2000). The asymmetric structure simulated is characterized by a highly-doped ( $1.6 \times 10^{18} \text{ cm}^{-3}$ ), narrow (70 nm)  $p^+$ -implant, located near the source end of the 250 nm channel of a conventional MOSFET, with substrate doping equal to  $10^{16} \text{ cm}^{-3}$  (Fig. 1).

Such a structure could, for instance, be realized by using focused ion beam implantation (FIBMOS) (Shen *et al.* 1998, Kang and Schroder 2000, Kang *et al.* in

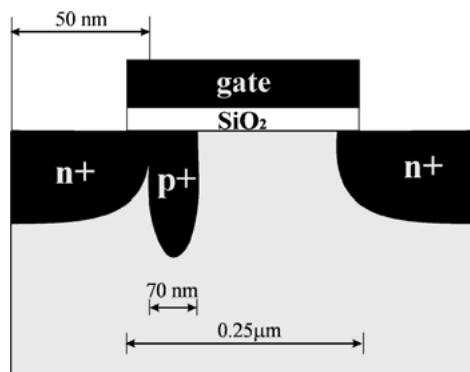


Figure 1. Schematic representation of the simulated asymmetric MOSFET structure.

press). There are several reasons for choosing such a structure: it is fairly easy to simulate, due to the simple geometry; the asymmetry effects should be observable because of the very abrupt changes in the doping profile, and the highly-doped implant region promises quantum effects even if the device as a whole is large.

The quantum effects in this study have been accounted for by including an effective potential (Ferry 2000) in the classical particle simulator. This has proven quite successful in treating the one-particle quantum effects in inversion layers (Ferry *et al.* 2000, Knezevic *et al.* 2002, Ramey and Ferry 2002). First, we will present the transfer characteristics of the device with and without the effective potential, and point out the main features that quantization introduces at the macro level of device analysis. We will then briefly review the microscopic quantum transport effects that have been known to contribute to the output trends obtained (Ferry *et al.* 2000, Knezevic *et al.* 2002, Ramey and Ferry 2002), and then focus on what has not received sufficient attention so far, and that is the behavior of low-field mobility when quantum effects are included in a highly asymmetric structure. The dependence of low-field mobility on the lateral electric field will be analyzed, with respect to both the introduction of asymmetry and quantum effects.

## 2. Macroscopic Signatures of Quantum Effects

The transfer characteristic of the simulated device structure with and without the inclusion of quantum effects, for the drain voltage  $V_D = 0.4$  V, is shown in Fig. 2. It is clear that the threshold voltage,  $V_{th}$ , is higher with the inclusion of the effective potential. Also, the device transconductance,  $g_m = dI_D/dV_G$ , in the linear

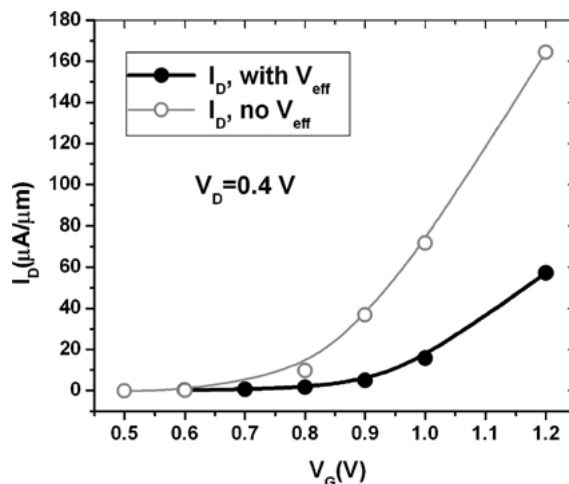


Figure 2. Transfer characteristic of the simulated asymmetric device structure, for drain bias  $V_D = 0.4$  V, with and without the inclusion of quantum effects through  $V_{eff}$ .

region is clearly lower if the effective potential,  $V_{eff}$ , is included.

It has been shown (Ferry *et al.* 2000, Knezevic *et al.* 2002, Ramey and Ferry 2002) that the inclusion of quantum effects in the microscopic description of the inversion layer of a metal-oxide-semiconductor device leads to two major features: reduced sheet density of channel carriers and charge set-back from the semiconductor/oxide interface. The reduced sheet density leads to an increase in the threshold voltage and a decrease in the drive current. On the other hand, the charge set-back leads to an effective increase in the oxide thickness, thereby degrading the device transconductance. Even though these two microscopic features undoubtedly have a very important impact on the transfer characteristics presented in Fig. 2, that may not be the entire story. Namely, there is very little change in the sheet density and the charge set-back between the equilibrium conditions and the non-zero drain bias situation, which means that these are virtually equilibrium quantum-mechanical effects. However, if the device is on and a bias is applied between the source and the drain, especially with an asymmetric doping profile such as that of the simulated device, some purely non-equilibrium features emerge.

## 3. Low-Field Mobility and the Interplay of Quantum Mechanics and Asymmetry

According to Fig. 2, the bias condition  $V_G = 1.2$  V with  $V_{eff}$  is almost equivalent to  $V_G = 1.0$  V without  $V_{eff}$ :

the current is similar, and  $V_G - V_{th}$  is virtually the same. Similarity is also noted between  $V_G = 1.0$  V with  $V_{eff}$  and  $V_G = 0.9$  V without  $V_{eff}$ . According to Fig. 3(a), which presents the profile of the effective perpendicular field in the channel for the above bias conditions, we indeed note that the equilibrium part of the quantum-mechanical influence, as described in the previous paragraph, is the same for  $V_G = 1.2$  V with and  $V_G = 1.0$  V without  $V_{eff}$ , and for  $V_G = 1.0$  V with and  $V_G = 0.9$  V without  $V_{eff}$ , so throughout this paper we will deal with these two pairs of bias conditions, as they will help us isolate the non-equilibrium signatures of quantum-mechanical effects.

By the effective field we mean the field felt by electrons, which is found according to

$$E_{eff}(x) = \frac{\int_0^{y_{max}} \mathbf{E}(x, y) n(x, y) dy}{\int_0^{y_{max}} n(x, y) dy}. \quad (1)$$

In (1),  $n$  is the electron concentration, the  $x$ -coordinate runs along the channel, starting at the source, and the  $y$ -axis is perpendicular to the semiconductor/oxide interface, starting at the interface and ending at the device bottom boundary ( $y_{max}$ ). This definition is meaningful only in inversion ( $n > 0$ ). (The effective field has nothing to do with the effective potential, despite the names.) Figure 3(b) shows the profile of the lateral effective field, while Fig. 3(c) presents the profile of the average carrier velocity in the channel. Note that the initially noisy raw Monte-Carlo output profiles have been smoothed.

The inclusion of the effective potential apparently leads to lower average velocity. Due to the pronounced asymmetry, the velocity overshoot is evident when the electrons just exit the implant and are subject to large negative electric fields. The inclusion of  $V_{eff}$  suppresses the overshoot. Also, at about 200–250 nm, we note that the lateral field is very low or even zero, whereas the velocity is finite, which signalizes that non-local effects are important (velocity is not correlated with the field at the given point), and transport can hardly be regarded as diffusive.

If the lateral field is low (and negative), below 10 kV/cm in magnitude, we can speak about low-field transport, and the low-field mobility profile along the channel can be found as

$$\mu(x) = \frac{v(x)}{E_{x,eff}(x)}. \quad (2)$$

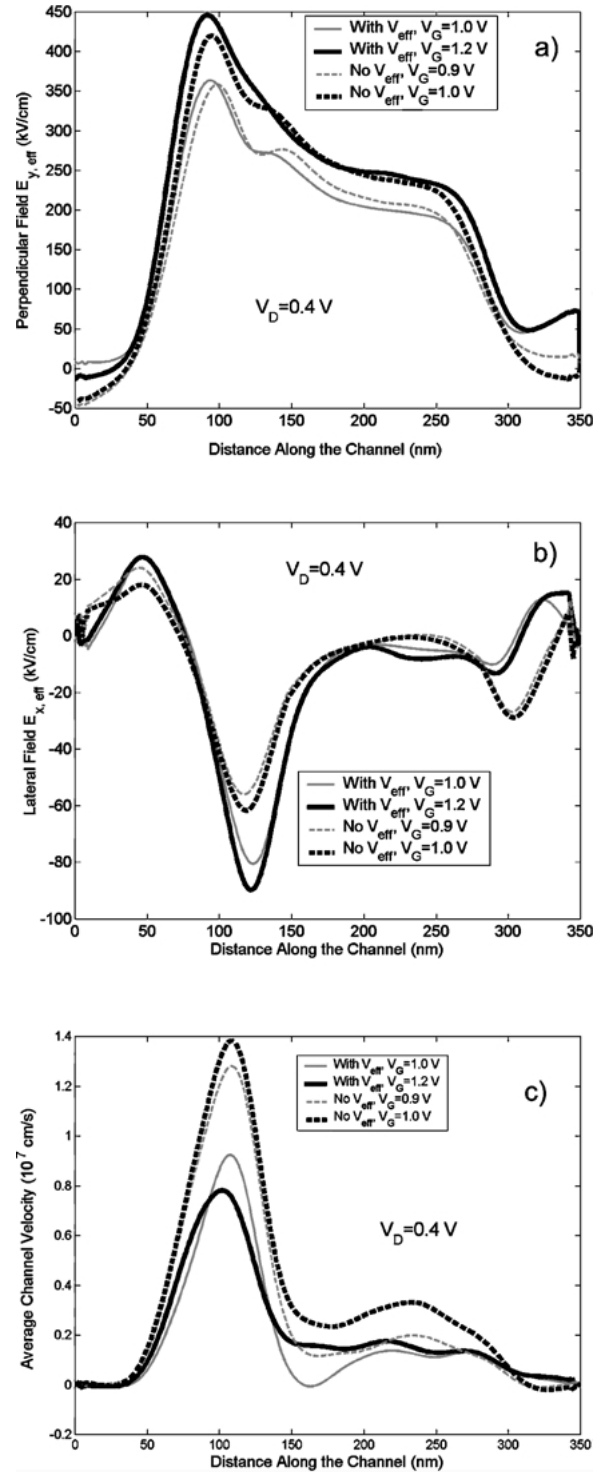


Figure 3. Profiles of the (a) perpendicular effective electric field, (b) lateral effective electric field and (c) average carrier velocity in the channel, with and without  $V_{eff}$ , for various gate bias conditions, and  $V_D = 0.4$  V.

The profiles  $E_{x,\text{eff}}(x)$ ,  $E_{y,\text{eff}}(x)$ ,  $\mu(x)$  obtained this way for a given  $V_D$ ,  $V_G$ , actually represent a parametric equation of a curve on the surface  $\mu(E_{x,\text{eff}}, E_{y,\text{eff}})$ . Even if we had infinitely many different bias conditions  $V_D$ ,  $V_G$ , we could never completely reconstruct the entire surface. However, we note that between 130 nm and 300 nm the perpendicular field is fairly monotonic, and if we restrict ourselves to the areas where the lateral field is monotonic as well, we are guaranteed that the curve  $(E_{x,\text{eff}}(x), E_{y,\text{eff}}(x), \mu(x))$  on the  $\mu(E_{x,\text{eff}}, E_{y,\text{eff}})$  surface gives single-valued projections onto  $E_{x,\text{eff}} = \text{const.}$  or  $E_{y,\text{eff}} = \text{const.}$  planes. After plotting  $(E_{x,\text{eff}}(x), E_{y,\text{eff}}(x), \mu(x))$  for regions between 130 nm and 300 nm with monotonic  $E_{x,\text{eff}}(x)$ , we find that the curve shows virtually no dependence on the perpendicular field within a given range of lateral fields. This is not surprising, as our simulation does not include surface roughness scattering, but only acoustic and intervalley phonon scattering. Therefore, we may conclude that

$$\mu(E_{x,\text{eff}}, E_{y,\text{eff}}) \approx \mu(E_{x,\text{eff}}(x)) \approx \langle \mu(E_{x,\text{eff}}) \rangle_{\text{averaged over all } E_{y,\text{eff}} \text{ in a given range}} \quad (3)$$

Figure 4 shows the low-field mobility as a function of the lateral field, for several values of the average perpendicular field as a parameter. As the lateral field approaches zero, the mobility increases, both with and without  $V_{\text{eff}}$ , which signals ballistic transport (in other words, non-locality; the retardation effects become important). However, the quantum mechanical behavior suppresses the ballistic feature. Even at

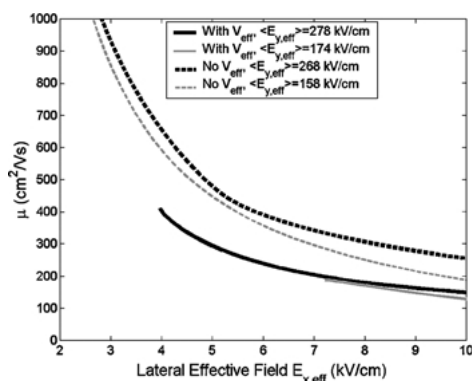


Figure 4. Variation of low-field mobility with the lateral effective field, with and without  $V_{\text{eff}}$ , for several perpendicular electric fields.

somewhat higher fields, the decrease in mobility due to the inclusion of  $V_{\text{eff}}$  is significant, which indicates that it is important to include the influence of quantum mechanical effects on mobility in order to have a realistic physical picture of device operation.

#### 4. Conclusions

In this paper we have investigated the influence of quantum-mechanical effects on low-field transport in a highly asymmetric MOSFET structure (Fig. 1). By analyzing the behavior with and without  $V_{\text{eff}}$ , we identified pairs of gate biases, such that one voltage in the pair corresponds to  $V_{\text{eff}}$  included and the other to  $V_{\text{eff}}$  excluded, and both lead to equivalent inversion conditions. Comparing between the two biases in the pair enables us to set aside the essentially equilibrium quantum mechanical effects, and just observe the non-equilibrium role of quantization in the simulated structure.

There are several important conclusions to be drawn. First, pronounced asymmetry leads to ballistic transport features. This feature is suppressed if the quantum-mechanical effects are included. Highly asymmetric devices therefore show signatures of ballistic transport, as seen also in the behavior of low field mobility. Even though quantum effects do lower the mobility, there is a definite tendency of mobility increase as the lateral field decreases, both with and without the effective potential. Altogether, asymmetry may lead to faster devices, but whether transport is truly ballistic or still diffusive needs to be carefully assessed by including quantum-mechanical effects into mobility modeling.

#### Acknowledgments

The authors would like to thank Massimo M. Fischetti, Steven M. Goodnick, Srdjan Milicic, Salvador Gonzalez and Gil Speyer for valuable discussions. Financial support from the Semiconductor Research Corporation, the Office of Naval Research under Contract No. N000149910318 and the National Science Foundation under NSF-CAREER ECS-9875051 is gratefully acknowledged.

#### References

- Buti T.N. *et al.* 1991. IEEE Trans. Electron Dev. 38: 1757.
- Ferry D.K. 2000. Superlattices Microstruct. 27: 61.

Ferry D.K. *et al.* 2000. IEDM Tech. Dig. 287.

Kang J. and Schroder D.K. 2000. In: Tech. Proc. of the Third International Conference on Modeling and Simulation of Microsystems, San Diego, California, March 27–29. p. 356.

Kang J. *et al.*, in press.

Knezevic I. *et al.* 2002. IEEE Trans. Electron Dev. 49: 1019.

Ma J. *et al.* 1997. IEEE Trans. Very Large Scale (VLSI) Syst. 5: 352.

Ramey S.M. and Ferry D.K. 2002. Physica B 314: 350.

Shen C.C. *et al.* 1998. IEEE Trans. Electron Dev. 45: 453.